LASER INTERFEROMETER GRAVITATIONAL WAVE OBSERVATORY
- LIGO -
CALIFORNIA INSTITUTE OF TECHNOLOGY
MASSACHUSETTS INSTITUTE OF TECHNOLOGY

LIGO-xxxxxxx-xx-x Feb. 28, 2012

GEO Squeezing Noise Budget

Kate Dooley, Hartmut Grote, Henning Vahlbruch (*alphabetical order for now*)

Distribution of this document:

LIGO Scientific Collaboration

Draft

California Institute of Technology
LIGO Project, MS 18-34
Pasadena, CA 91125
Phone (626) 395-2129
Fax (626) 304-9834
E-mail: info@ligo.caltech.edu

Massachusetts Institute of Technology
LIGO Project, Room NW17-161
Cambridge, MA 02139
Phone (617) 253-4824
Fax (617) 253-7014
E-mail: info@ligo.mit.edu

LIGO Hanford Observatory
Route 10, Mile Marker 2
Richland, WA 99352
Phone (509) 372-8106
Fax (509) 372-8137
E-mail: info@ligo.caltech.edu

LIGO Livingston Observatory
19100 LIGO Lane
Livingston, LA 70754
Phone (225) 686-3100
Fax (225) 686-7189
E-mail: info@ligo.caltech.edu

http://www.ligo.caltech.edu/

Table 1: OMC parameters. Many numbers come from p.12 of the GEO-HF logbook.

quantity	symbol	value	units
Finesse	F	160	
round trip length	L	0.658	m
g-factor	g	0.735	
waist size	ω_0	450	µm
free spectral range	FSR	455.6	MHz
Michelson sideband power transmission	T_{MI}	1.01	%
SRC sideband power transmission	T_{SR}	2.71	%

1 Introduction

....

2 Overview of squeezing setup

3 OMC parameters

Table 1 summarizes the OMC design parameters. Note that the sideband transmission numbers (T_{MI} and T_{SR}) should be doubled in practice to account for the existence of both upper and lower sidebands.

4 Optical losses

Table 2 summarizes our optical loss budget for the squeezer path. We find that only 64% of the squeezed light sent into the interferometer makes it to the detection PD. This optical loss immediately reduces the maximum possible observed squeezing from 10 dB to 4 dB (make figure!).

5 Phase noise from RF sidebands

The presence of both the carrier contrast defect and the RF sidebands in the OMC transmitted light results in jitter of the squeezing quadrature. Figure 2 provides a pictorial view of the role of the sidebands in modulating the fields at the output port. The carrier field itself is only amplitude modulated by the sidebands, so if were the only field after the OMC, the

Table 2: Optical losses of squeezed beam.

component	power loss	notes
squeezer path Faraday	3.3%	
output port Faraday	3.3%	guess, experienced twice
BDO1 transmission	1%	experienced twice
MSR transmission (when locked)	1%	above 1 kHz
OMC mode-matching loss	6%	
OMC AR coating loss	1%	
OMC internal losses	14%	deduced from other measurements
OMC trans PD detection loss	9%	
TOTAL	63.9%	multiplied in series

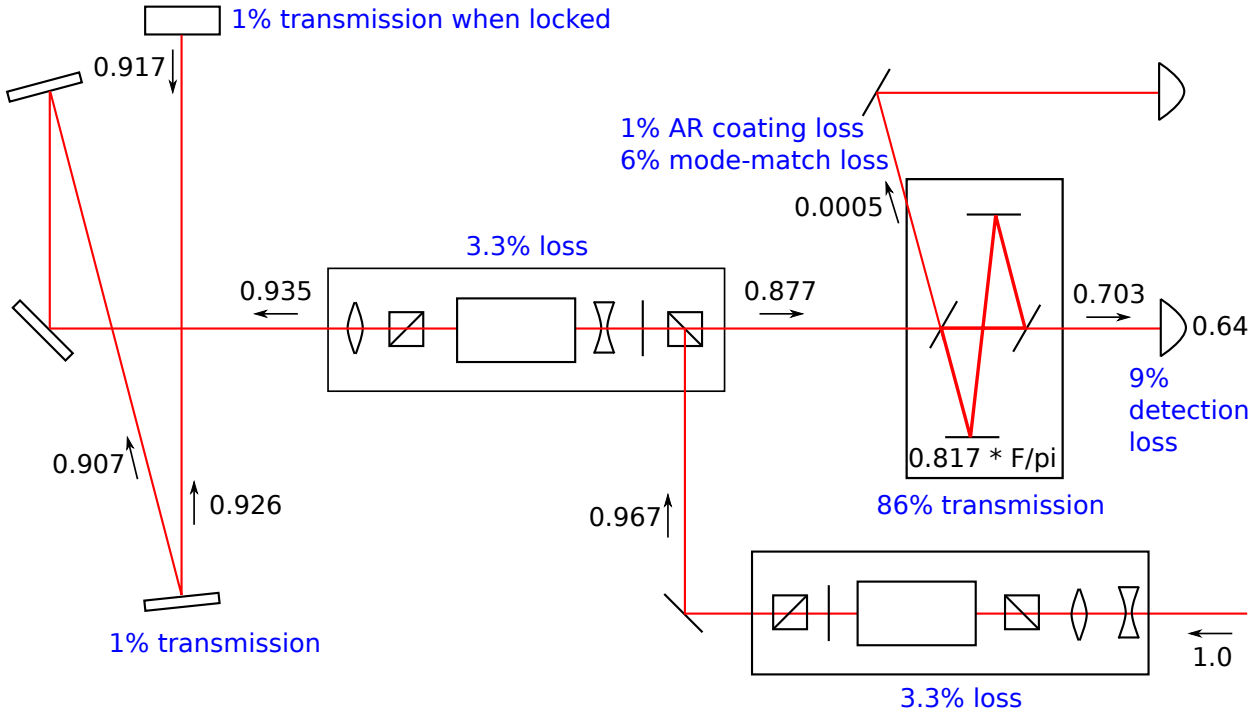

Figure 1: Optical losses in the squeezer path.

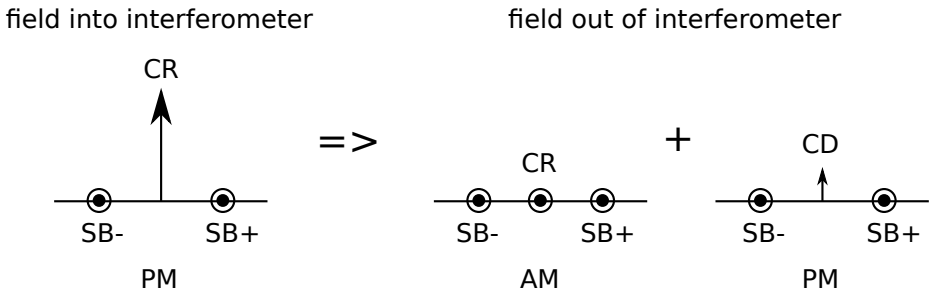

Figure 2: The RF sidebands (SB+ and SB-) are generated via phase modulation of the carrier field. The Michelson interferometer rotates the differential carrier field (CR) by 90°, but leaves all other fields the same, including the RF sidebands and the contrast defect (CD). The result is that at the output port, the RF sidebands are amplitude modulation (AM) on the carrier, yet continue to be phase modulation (PM) on the contrast defect.

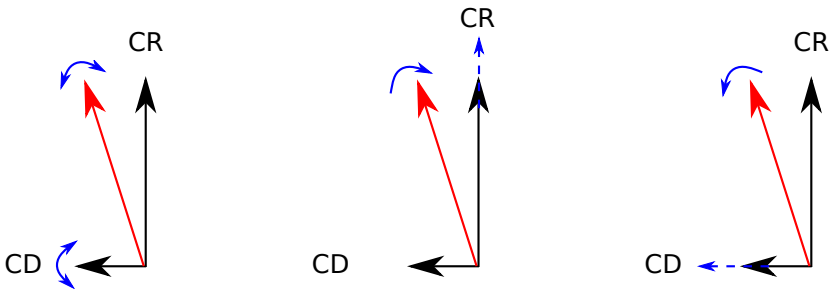

Figure 3: Examples of how jitter of the squeezing quadrature is generated.

squeezing quadrature angle would not change. In the presence of other fields, the squeezing quadrature is determined by the sum of the fields. Changes in the quadrature angle are created in three ways:

- phase noise on the contrast defect
- amplitude noise on the carrier when contrast defect is present
- amplitude noise of the contrast defect (due to changing ifo thermal states)

Figure 3 shows phasors demonstrating these three situations.

Rewriting Eq. 90 from T0900325, the rms fluctuation of the squeezing quadrature angle, $\Gamma_{\rm rms}$, is dependent on the ratio of carrier light with signal, $P_{\rm CR}$, to light without signal that is transmitted through the OMC. Examples are the contrast defect carrier, $P_{\rm CD}$, and the sidebands, $P_{\rm SB}$:

$$\Gamma_{\rm rms} = \sqrt{\frac{P_{\rm SB}}{P_{\rm CR}}\left(\frac{1}{\eta} + \epsilon^2\frac{1-\eta}{\eta}\right)} \tag{1}$$

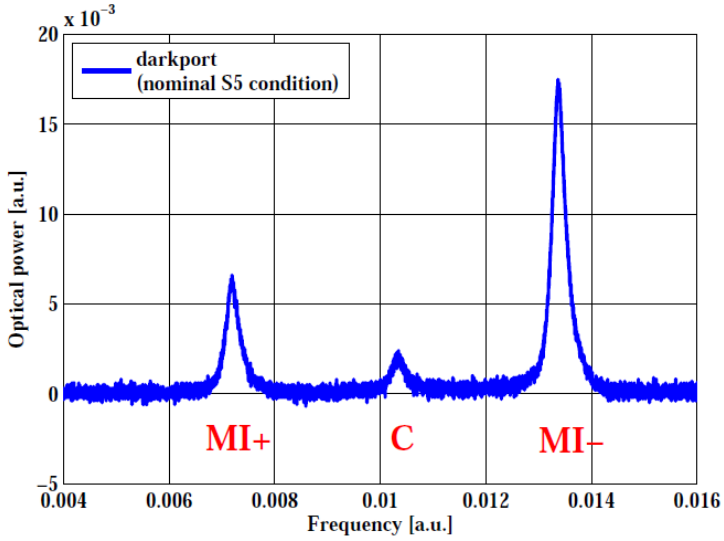

Figure 4: Snapshot of a scan of the output port by Stefan Hild (thesis) showing the sideband imbalance. In this particular plot, $\epsilon = 0.23$. It was more recently measured to be $\epsilon = 0.15$.

All powers in this equation are for those transmitted through the OMC, and the variables η and ϵ are defined as follows:

$$\eta = \frac{P_{\mathrm{CR}}}{P_{\mathrm{CD}}} \tag{2}$$

$$\epsilon = \frac{1}{2}\frac{P_{\mathrm{SB+}} - P_{\mathrm{SB-}}}{P_{\mathrm{SB+}} + P_{\mathrm{SB-}}} \tag{3}$$

The sideband imbalance is quantified by ϵ and a sample measurement of the imbalance (from several years ago) is shown in Figure 4. Currently, $\epsilon = 0.15$. The contrast defect, commonly quoted as $1/\eta$, can be measured by comparing the power transmitted through the OMC with and without the dark fringe offset. It arises from asymmetry in the reflectivity of each arm and is approximately 5%.

Figure 5 shows the dependence of phase noise on contrast defect for our current sideband imbalance. We expect an rms phase noise of about 2°.

5.1 Manipulating Γ_{rms}

We changed the rms phase noise up to a factor of 4 by reducing the sideband amplitude and increasing the dark fringe offset. The result is an improvement in the observed squeezing from 1.9 dB to 2.8 dB.

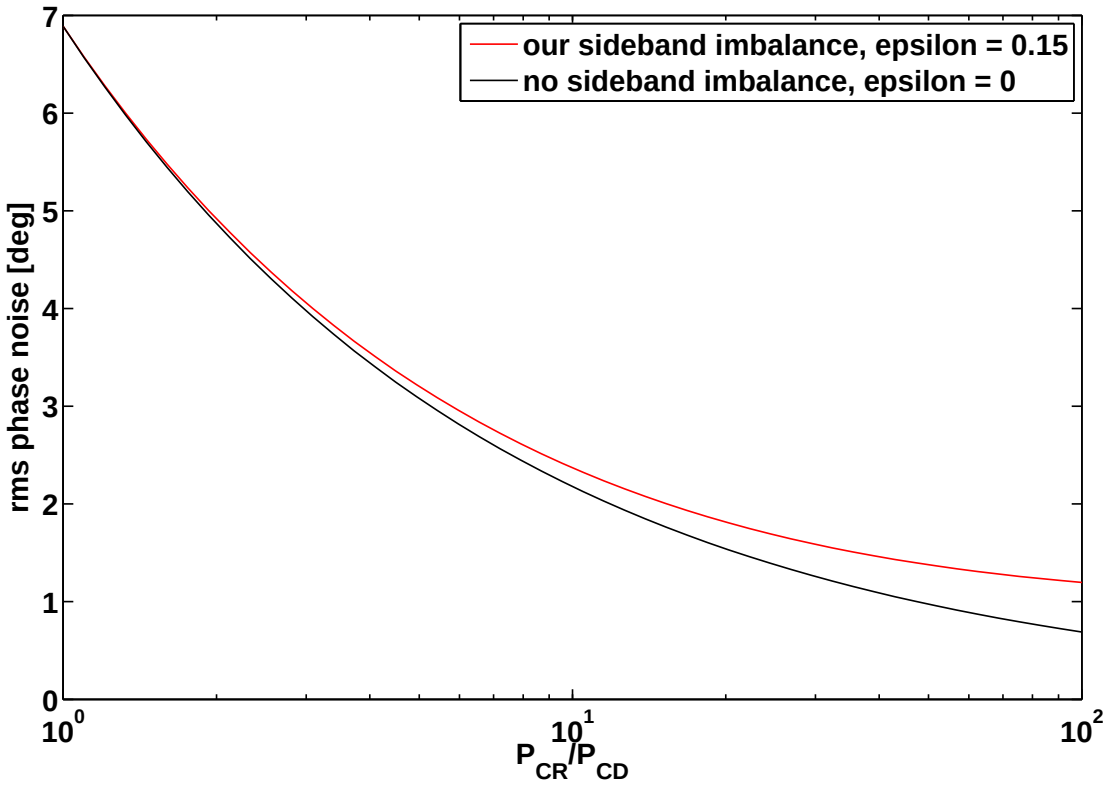

Figure 5: RMS phase noise as a function of the ratio of carrier to contrast defect in the OMC transmitted beam. The typical operating point for GEO is $P_{\mathrm{CR}}/P_{\mathrm{CD}} = 20$, which corresponds to an RMS phase noise of 1.8°.

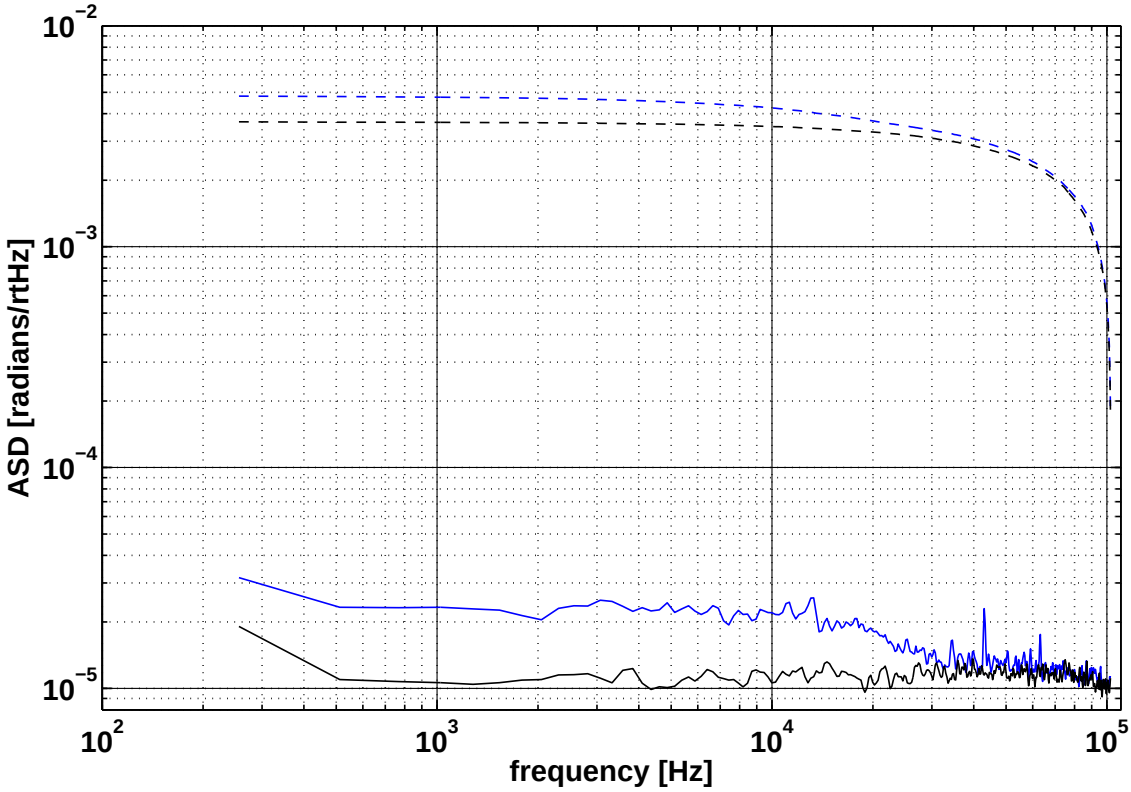

Figure 6: Calibrated squeezer error point (blue curve), measured as the beat between the squeezer sidebands and the RF Michelson sidebands in reflection of the OMC. We are limited by dark noise (black curve) above 40 kHz. (verify calibration)

5.2 Squeezer phase error point

Our current setup for creating a squeezer to GEO output relative phase error signal uses the beat of the squeezer sidebands with the Michelson sidebands in reflection of the OMC which are at 15.2 MHz and 14.9 MHz, respectively. A sample error point spectra is shown in Figure 6 and demonstrates that we measure only 5 mrad rms phase noise. Our sensor is not measuring the 35 mrad ($\approx 2^\circ$) predicted by the RF sideband model of Eq. 1.

5.3 Contrast defect

We implement a slow servo called the *noiselock loop* that serves to change the squeezing quadrature in order to maximize the strain sensitivity. The need for such a servo (??) arises from the existence of contrast defect carrier in the OMC transmitted beam. When the

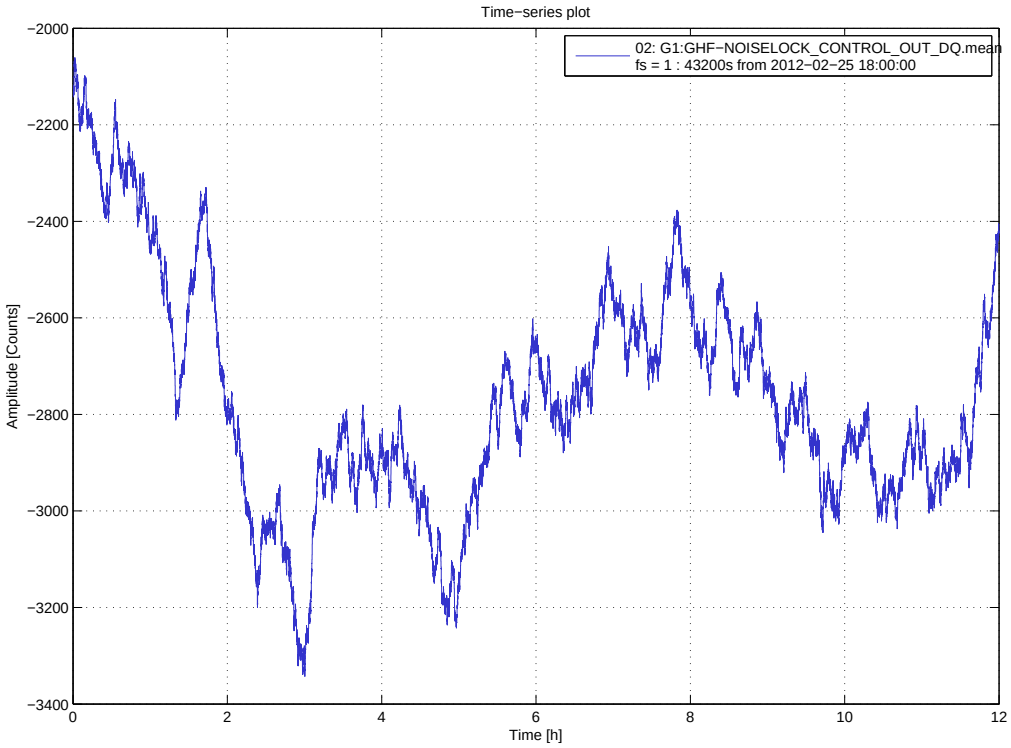

Figure 7: Example of drift of squeezer demodulation phase over the course of 12 hours. Calibrate to radians!

amplitude of the contrast defect changes in time, so does the angle of the quadrature that produces the best squeezing. An example of how much drift we observe is shown in Figure 7.

6 Higher order modes

We plan to test the effect of higher order modes on the squeezing quadrature jitter by placing an aperture in the beam path after the OMC.

Based on the OMC finesse, g-factor and FSR, we can calculate the amount of higher order modes that are transmitted. Table 3 shows that of the first 5 HOMs, $n + m = 5$ sits closest to the fundamental mode and 0.06% of what's incident on the OMC is transmitted.

This does not reflect any coupling of higher order modes into the OMC fundamental mode as a result of poor alignment. We can place an upper limit on the contribution of higher order modes to squeezer phase noise through experiments with changing the sideband and dark fringe offset powers.

Table 3: OMC mode spacing

HOM order $(n+m)$	1	2	3	4	5
transmission factor (%)	0.041	0.014	0.011	0.016	0.061

7 Ideas for improvements

1. 2nd OMC
2.

8 Acknowledgements